

WIT2012 — WORKSHOP ON INTELLIGENT TRACKERS,
 3–5 MAY 2012,
 INFN PISA, ITALY

FTK: a Fast Track Trigger for ATLAS

J. Anderson,^f A. Andreani,^{m,n} A. Andreazza,^{m,n} A. Annovi,^b M. Atkinson,^e
 B. Auerbach,^f M. Beretta,^b V. Bevacqua,^{a,c} R. Blair,^f G. Blazey,^q M. Bogdan,^d
 A. Boveia,^d F. Canelli,^{d,j} A. Castegnaro,^b V. Cavaliere,^e F. Cervigni,^r P. Chang,^e
 Y. Cheng,^d M. Citterio,^m F. Crescioli,^{a,c} M. Dell'Orso,^{a,c} G. Drake,^f M. Dunford,^d
 L. Fabbri,^{o,p} A. Favareto,^{m,n} M. Franchini,^{o,p} S. Geer,^j P. Giannetti,^a F. Giannuzzi,^{o,p}
 F. Giorgi,^o S. Gruenendahl,^j H.-L. Li,^d J. Hoff,^j T. Iizawa,^h O. Jamieson,^j A. Kapliy,^d
 M. Kasten,^e Y.K. Kim,^{d,j} N. Kimura,^h A. Lanza,^k F. Lasagni,^{o,p} V. Liberali,^{m,n} T. Liu,^j
 D. Magalotti,^{b,r} A. McCarn,^e C. Melachrinou,^d C. Meroni,^m T. Mitani,^h P. Murat,^j
 A. Negri,^{l,k} M. Neubauer,^e Y. Okumura,^{d,j} B. Penning,^{d,j,1} M. Piendibene,^{a,c}
 J. Proudfoot,^f C. Roda,^{a,c} I. Sacco,^t Y. Sakurai,^h C. Sbarra,^o M. Shochet,^d
 A. Stabile,^{m,n} J. Tang,^d F. Tang,^d L. Tompkins,^d R. Tripiccione,^g J. Tuggle,^d
 S. Valentinetti,^{o,p} V. Vercesi,^k M. Verzocchi,^j M. Villa,^{o,p} G. Volpi,^{b,d} J. Webster,^d
 K. Yorita,^h J. Zhang,^f and A. Zoccoli^{o,p}

^aSezione di Pisa, INFN, Pisa, Italy

^bLaboratori Nazionali, INFN, Frascati, Italy

^cDepartment of Physics, University of Pisa, Pisa, Italy

^dDepartment of Physics and Enrico Fermi Institute, University of Chicago, Chicago, Illinois, U.S.A.

^eDepartment of Physics, University of Illinois at Urbana-Champaign, Urbana, Illinois, U.S.A.

^fArgonne National Laboratory, Argonne, Illinois, U.S.A.

^gDepartment of Physics, University of Ferrara, Ferrara, Italy

^hDepartment of Physics, Waseda University, Waseda, Japan

ⁱDepartment of Physics, University of Harvard, Harvard, Massachusetts, U.S.A.

^jFermi National Accelerator Laboratory, Fermilab, Batavia, Illinois, U.S.A.

^kSezione di Pavia, INFN, Pavia, Italy

^lDepartment of Physics, University of Pavia, Pavia, Italy

^mSezione di Milano INFN, Milan, Italy

ⁿDepartment of Physics, University of Milan, Milan, Italy

¹Corresponding author.

^a*Sezione di Bologna INFN, Bologna Italy*

^b*Department of Physics, University of Bologna, Bologna, Italy*

^c*Northern Illinois University, DeKalb, Illinois, U.S.A.*

^d*Department of Physics, University of Perugia, Perugia Italy*

^e*University of Copenhagen, Copenhagen, Denmark*

^f*Institute of Computer Engineering, University of Heidelberg, Heidelberg, Germany*

E-mail: penning@cern.ch

ABSTRACT: We describe the design and expected performance of a the Fast Tracker Trigger (FTK) system for the *ATLAS* detector at the Large Hadron Collider. The FTK is a highly parallel hardware system designed to operate at the Level 1 trigger output rate. It is designed to provide global tracks reconstructed in the inner detector with resolution comparable to the full offline reconstruction as input of the Level 2 trigger processing. The hardware system is based on associative memories for pattern recognition and fast FPGAs for track reconstruction. The FTK is expected to dramatically improve the performance of track based isolation and *b*-tagging with little to no dependencies of pile-up interactions.

KEYWORDS: Trigger concepts and systems (hardware and software); Trigger algorithms

Contents

1	The FTK system	1
1.1	The ATLAS detector and trigger	1
2	Technical design	2
2.1	Overview	2
2.2	Pattern recognition and track fitting	3
2.3	Variable resolution patterns	4
3	Physics with the FTK	4
3.1	Simulated performance	5
4	Conclusion	5

1 The FTK system

The FTK [1] is a trigger upgrade for the ATLAS detector at the Large Hadron Collider (LHC). As the LHC luminosity approaches its design luminosity of $10^{34}\text{cm}^2/\text{s}$, the combinatorial problem arising from charged particle tracking becomes increasingly difficult, resulting in lower signal efficiencies for constant fake rates for larger pile-up. The FTK is a highly-parallel hardware system intended to provide high-quality reconstruction of all tracks with transverse momentum above 1 GeV. Its speed and physics performance have been estimated at simulated luminosities up to $3 \times 10^{34}\text{cm}^2/\text{s}$, corresponding to 75 interactions per bunch crossing at a bunch crossing interval of 25 ns. An overview of the ATLAS detector and trigger system is given in the following section, followed by details of pattern recognition, track fitting and physics performance.

1.1 The ATLAS detector and trigger

ATLAS is one of the two general-purpose detectors at the LHC [2]. It is designed to detect particles produced in proton-proton collisions at a center of mass energy of $\sqrt{s} = 14\text{ TeV}$. Particles are detected (moving from the interaction point) by the inner tracking system, followed by the electromagnetic and the hadronic calorimeters, and at the end by the muon system. ATLAS collected in the years 2010 – 2011 5.3 fb^{-1} of data with an energy of $\sqrt{s} = 7\text{ TeV}$. Peak luminosities of about $3.5 \times 10^{33}\text{cm}^2/\text{s}$ have been achieved. In 2012 the LHC energy is increased to $\sqrt{s} = 8\text{ TeV}$ with peak luminosities exceeding $6 \times 10^{33}\text{cm}^2/\text{s}$. The inner detector consists of the Pixel detector, the Semiconductor Tracker (SCT) and the Transition Radiation Tracker (TRT). The inner tracker is inside a 2 T solenoidal magnetic field. The Pixel detector system contains 80 M channels of $50 \times 400\ \mu\text{m}^2$ silicon pixels. These are arranged in three cylindrical layers with radii of 5, 9 and 12 cm with three disks on each side, located at distances of 495, 580 and 650mm in z and covering a radial region of 9 and 15 cm. Typically each track traverses three Pixel layers up to $|\eta| < 2.4$. The ATLAS detector

will be upgraded by installation of an additional Pixel Detector layer. The new layer will be inserted between the B-layer of the existing pixel detector and a new smaller radius beam-pipe. The SCT system consists of 4 double layer of silicon strip detectors. Each double layer has an axial- and a stereo layer with $80\ \mu\text{m}$ pitch, oriented along the beam direction (axial) in one layer and tilted by $40\ \text{mrad}$ angle (stereo) in the second one. The entire SCT has 6M channels and consists of cylinders at radii of 30.0, 37.3, 44.7, and 52.0 cm. The end-cap modules are very similar in construction but use tapered strips aligned radially. The FTK uses all 3 Pixel and 4 SCT double layers mapped into 11 logical layers. Use of the insertable B-layer is anticipated, too. The rapidity coverage extends up to $|\eta| < 2.5$. Details regarding the inner detector are given in ref. [2].

A three level trigger system [3] is used to select interesting events. The first level is hardware-based, operating at a maximum output rate of 100 kHz. It provides regions of interest, portions of the detector in azimuth and pseudorapidity, which causes the event to trigger. Level 2 and the Event Filter are build by using computing farms and are collectively known as the High Level Trigger (HLT). The HLT consists of several thousand CPUs. Level 2 operates within regions of interest with an output rate of 2 kHz, while the Event Filter has access to all information in the event, with an output rate of 200 Hz.

2 Technical design

2.1 Overview

The FTK system core design is based on the experience of the Silicon Vertex Trigger at the CDF detector at Fermilab [7, 8]. The system is based on FPGAs and a highly-parallel Associative Memory (AM) chip [9]. The system is divided into eight core crates, each covering a 45° range in azimuth plus 10° overlap. Each core crate is further divided into four regions of η and two regions in ϕ . This yields $8\ \eta - \phi$ towers per crate and 64 trigger towers altogether. A $\eta - \phi$ tower is served by two processing units containing the AM chips for pattern recognition, Track Fitters (TF), Data Organizers (DO) to coordinate between pattern recognition and track fitting, and a Hit Warrior (HW) to remove duplicate tracks from the output. The processing units receive inputs from Data Formatter (DF) boards and pass their output to second stage boards which perform final full resolution track fitting and quality tests. Each of these components are described below. A sketch is given in figure 1.

Dual output front end links (RODs in figure 1) from the silicon detectors direct a duplicate set of the output to the Data Formatter boards which perform hit clustering and formatting of the data to be mapped to the 11 logical layers of the FTK architecture. Then it routes the clusters to the relevant processing units. In each processing unit the Data Organizer reduces the cluster resolution by a factor ≈ 10 into superstrips used for pattern recognition while storing the full resolution clusters for track fitting. The superstrips then are passed to the AM chips. Those operate in parallel to compare the incoming superstrips to approximately 100 million precomputed patterns per core crate. Matched patterns are sent back to the DO, which retrieves the full resolution hits and sends them to the Track Fitter. The TF does linear calculations of the helix parameters and χ^2 components using prestored constants and the location of the hit in each layer. Every combination of hits within a given pattern is fitted; those passing a fit-quality criteria are kept. The last stage of each processing unit is the Hit Warrior which removes duplicate tracks based on the number of shared hits between various tracks and the χ^2 of the fit.

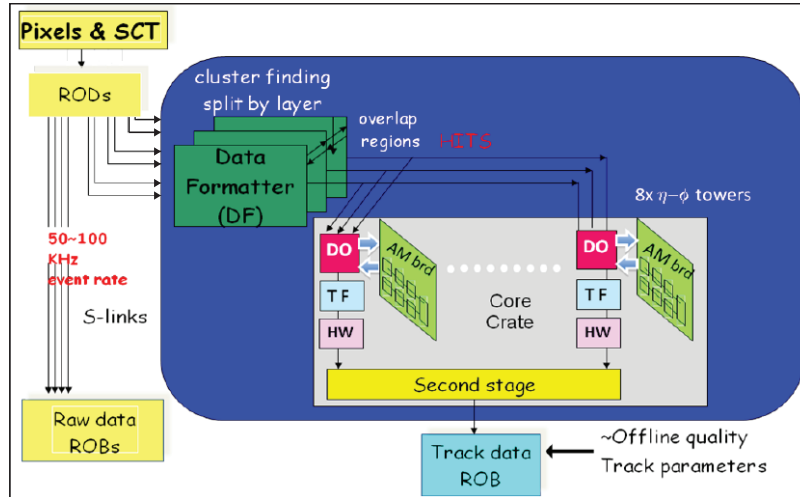


Figure 1. Sketch of the FTK system [1].

2.2 Pattern recognition and track fitting

FTK tracking is performed in two stages to keep the combinatorics at a manageable level. The first stage uses 8 out of 11 silicon layers for pattern recognition and track fitting while the second stage refits the tracks found in the first stage using all 11 layers. The first 8 layer stage uses 3 Pixel, 4 axial SCT and 1 stereo SCT layer. At least seven of eight layers are required to have a hit. The pattern matching takes place in CAM-based custom built AM chips, each containing 50k-100k patterns each. Hits entering the system are simultaneously compared to all stored patterns. The AM chips are grouped in sets of 32 chips on a local associative memory board (LAMB). Each AM board contains four LAMBs. Once all matched patterns, called roads, in an event are found the information is sent back to the DO. The DOs are located on an auxiliary (AUX) card attached to the AM board. Each AUX card has four instances of the Data Organizer, Track Fitter and Hit Warrior. Upon receiving the roads from a LAMB, the Data Organizer looks up the full resolution hits within a road and sends them to the Track Fitter. The TF unit is expected to fit one track per nanosecond. This high rate is achieved by the large numbers of DSPs in the FPGA used to perform a simple linear fit for each set of N hit coordinates x_j :

$$p_i = \sum_j^N c_{ij} x_j + q_i \quad (2.1)$$

The p_i are the five helix parameters and the $N - 5 \chi^2$ components, all of which are determined from the constants c_{ij} and q_j . If a fit is above a given χ^2 threshold and the candidate track has hits in all the detector layers, a majority recovery is performed. During this recovery the track is refitted several times, ignoring one of the hits each time to check whether a subset of hits will yield a good χ^2 . This allows a track to be recovered if one of the hits in the combination comes from noise or from a different track. The second stage of fitting uses the good tracks from the first stage to look for expected hits in the remaining 3 layers, using an inversion of eq. (2.1). If at least 10 out of 11 hits are found, the track is refit with all of the hits and subjected to a final fit quality test. The tracking process takes in average about 15 μ sec.

2.3 Variable resolution patterns

One of the challenges in the design of the FTK is the large number of matched roads expected at $3 \times 10^{34} \text{cm}^2/\text{s}$. Although the system is already segmented into independently operating $\eta - \phi$ towers, the number of matched roads out of the AM could still be a challenge for the Data Organizer at very high instant luminosities and better pattern matching resolution could be necessary. Variable-resolution patterns have been developed to obtain better resolutions with equal AM bank sizes or the same resolution with much smaller banks [10]. Finer-resolution patterns lead to a lower fake rate at the cost of more required AM space, while coarse resolution maintains higher efficiency at the cost of increased combinatorics in the Track Fitter. The solution described here maintains a balance between these considerations. The logic of the AM chip design has been upgraded to include local subdivisions of each superstrip in a pattern.

The “don’t care” feature of modern CAMs is implemented so that the width of each pattern can be varied layer by layer. This allows the available hardware pattern space to be optimized to maximize efficiency while minimizing the number of random hits that have to be fit.

Simulation studying events with different pile-up conditions have been performed. A standard AM bank produces roughly the same number of roads of a variable resolution pattern bank that is 3–5 times smaller when using a single DC bit in the AM logic [10]. At the level of 70 pile-up, a fairly uniform 900–1300 clusters are expected per layer and tower.

3 Physics with the FTK

There is a variety of physics applications for the FTK. One of the most prominent is the source of electroweak symmetry breaking which remains yet unknown. The easiest explanation, the Higgs mechanism [4–6], predicts the Higgs boson whose branching ratios to other particles are dependent on their masses. Therefore the production of heavy particles like b -quarks and τ leptons are of particular interest. These couplings can be modified by new physics and their measurement is a crucial test for the Standard Model. We will show that particularly for these final states the FTK system leads to significant improvements. In Standard Model measurements the FTK helps to maintain high efficiencies while controlling background processes at high pile-up.

Figure 2, left, shows the isolated muon efficiency using the EM calorimeter isolation with two different cell energy thresholds as function of the number of pile-up interactions. The selection criteria are chosen such that the $b\bar{b}$ rejection factor is 10. The second plot of the same figure demonstrates that by applying tracking isolation in contrast to calorimeter isolation the efficiency improves. Considering only tracks from the muon vertex by applying a selection criteria on the distance between muon and track at the beamline track the efficiency becomes largely independent of the pile-up. These examples demonstrate that tracking can play an important role in identification of interesting events while maintaining high efficiency. With increasing luminosity the use of tracking increases even more. The FTK will operate at the Level 1 trigger output rate, reconstructing all tracks at near-offline quality for use in the HLT. In addition this frees up CPU time in the HLT, which can be used for other purposes.

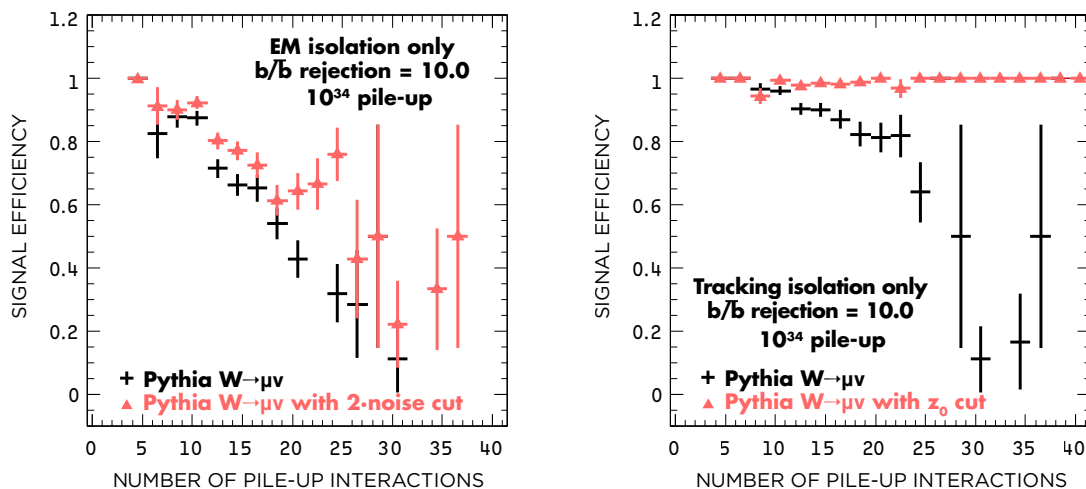


Figure 2. Left: Isolated muon efficiency using the EM calorimeter isolation with two different cell energy thresholds as a function of the number of pile-up interactions, for a fixed $b\bar{b}$ rejection factor of 10. Right: Isolated muon efficiency using track isolation with and without a cut on the distance between the track and the muon at the beamline as a function of the number of pile-up interactions, for a fixed $b\bar{b}$ rejection factor of 10. Signal efficiency here gives the efficiency to select isolated muons. Figures from [1].

3.1 Simulated performance

The FTK system has been simulated in software to determine its expected performance [1]. Tracks provided by the FTK system are compared with tracks reconstructed using the ATLAS offline tracking algorithm. The resolution of track parameters is shown in figure 3 for tracks with $|\eta| < 1$, demonstrating that the FTK resolution is comparable to that of the offline tracking.

The FTK configuration uses collections of pre-calculated pattern (pattern banks) and linearized fitting constants suitable for up to 75 pile-up interactions. Figure 4 shows the efficiency of the FTK and offline algorithm to reconstruct muons of $p_T > 1$ GeV. The efficiency drops for FTK tracks around pseudorapidity $\eta = 1$ are located at the transition region between barrel detector and forward disks. These have been addressed by relaxing the number of hits required in these particular regions.

The potential for heavy flavor identification (b -tagging) with the FTK tracks at high luminosities is evaluated using an algorithm based on the transverse impact parameter d_0 of tracks in jets. Template histograms of the impact parameter divided by its uncertainty are created for light jets and b jets. These are combined to form a likelihood. Figure 5 shows the expected b -quark efficiency along with typical light jet rejection factor for FTK and offline tracks. Simulated event samples are $WH \rightarrow b\bar{b}$. Typical b -tagging efficiencies used in analyses are ~ 0.5 – 0.7% .

4 Conclusion

The Fast Track Trigger for ATLAS will be able to increase efficiency and control background processes for particularly interesting events containing b quarks, τ leptons and isolated, high p_T electrons and muons. This is achieved by using global, high speed tracking at the beginning of the

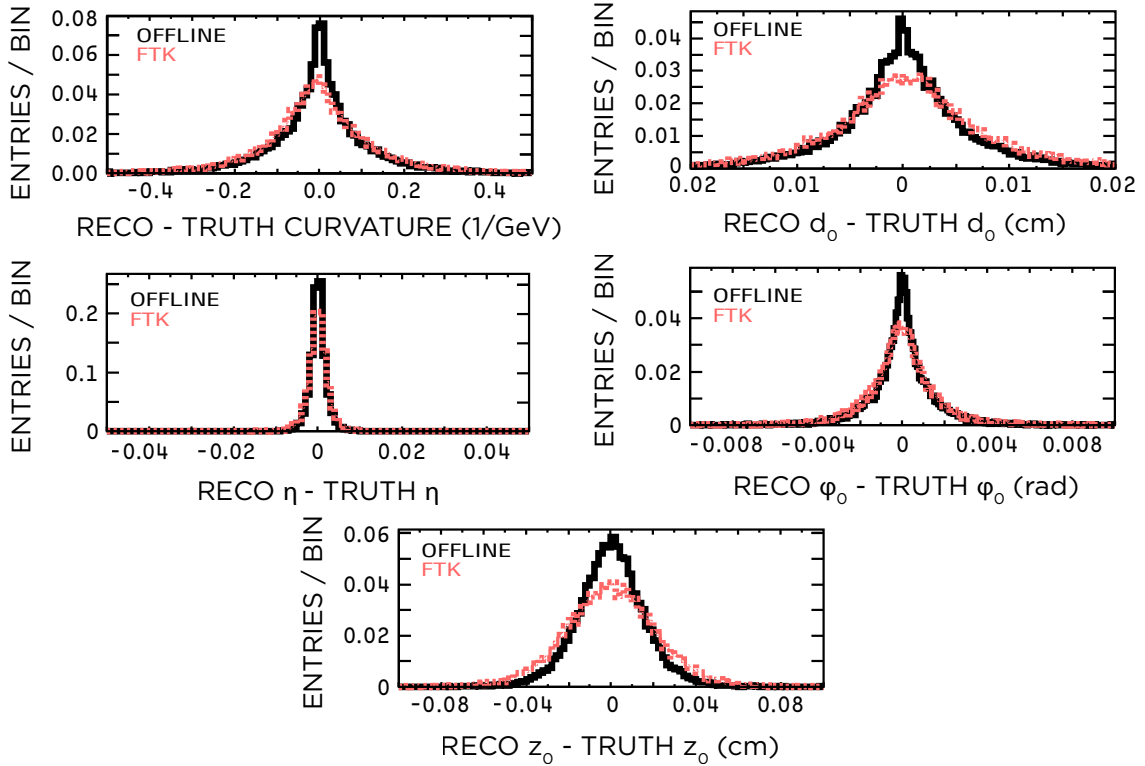


Figure 3. Comparison of the helix parameters for Offline track reconstruction (black) and FTK (red). The track's transverse momentum is required to exceed 1 GeV and its pseudorapidity is limited to the central region ($|\eta| < 1$). A single muon sample is used. Figure from [1].

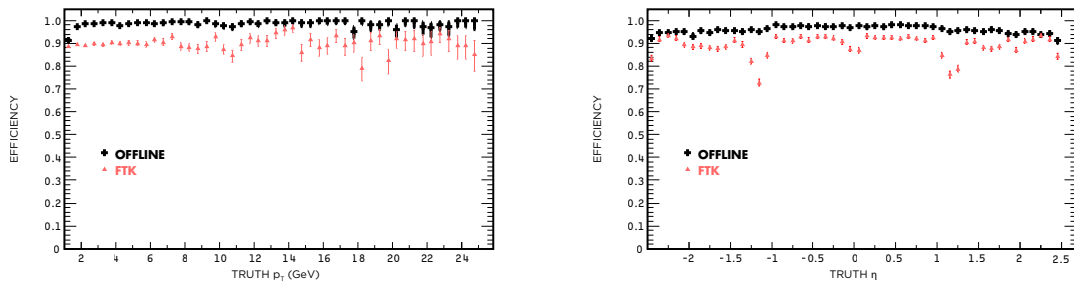


Figure 4. Comparison between single muon tracking efficiencies for FTK and offline algorithms vs. p_T (left) and η (right). Figures from [1].

Level 2 trigger. The challenges given by increased combinatorics in track reconstruction with increasing luminosity and simultaneously greater need for computational power are solved by using precomputed AM based patterns and fast FPGAs in a highly parallel system.

A vertical slice test using collision data in summer 2012 is in preparation [11]. The dual output silicon detector front end cards needed are already installed in ATLAS. The full set of dual output cards for the final system is already produced. A data formatter prototype board is currently under design and will be ready by summer 2012. A prototype input mezzazine [12] is ready for

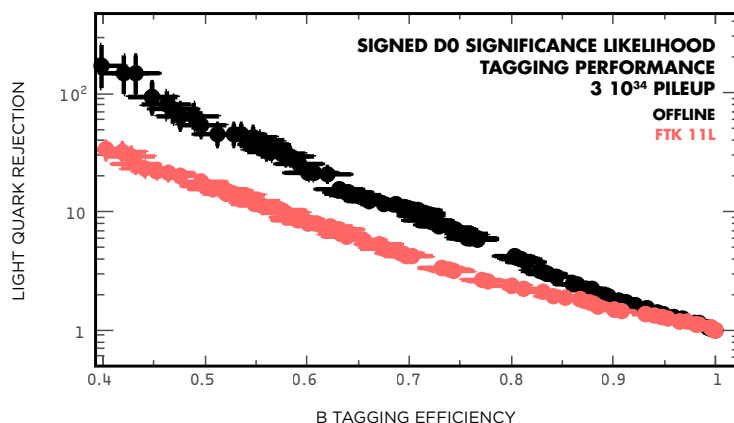


Figure 5. Light-quark jet rejection vs b-quark jet efficiency for offline and FTK tracks at pile-up as expected for a luminosity of $\approx 3 \times 10^{34}$. The FTK simulation uses as configuration of 11 layer (11L). Figure from ref. [1].

the vertical slice test. The AM chip prototype (AMchip04) is expected by early summer 2012 and the design of the AM board (AMBFTK) is finished. An existing board (AMBslim5) [13] will be used for the vertical slice test. For the data organizer board a pre-prototype is available and will be used in high-speed testing. The second stage board which performs the full 11 layer fit is currently undergoing conceptual design and firmware development. We expect the system to be operational in the data taking period following the 2013-2014 shutdown.

Acknowledgments

The author thanks the organizers of the WIT2012 workshop for the invitation, the FTK collaboration and TDAQ speakers committee for their advise preparing the presentation and these proceedings. The Fast Tracker project receives support from Istituto Nazionale di Fisica Nucleare, from the US Department of Energy and National Science Foundation, from Grant-in-Aid for Scientific Research by Japan Society for the Promotion of Science, from European community FP7 (Marie Curie OIF Project 254410 - ARTLHCFE).

References

- [1] A. Andreani et al., *The fast tracker real time processor and its impact on muon isolation, tau and b-jet online selections at ATLAS*, *IEEE Trans. Nucl. Sci.* **59** (2012) 348.
- [2] ATLAS collaboration, G. Aad et al., *The ATLAS experiment at the CERN Large Hadron Collider*, 2008 *JINST* **3** S08003.
- [3] ATLAS collaboration, G. Aad et al., *Expected performance of the ATLAS experiment — detector, trigger and physics*, [arXiv:0901.0512](https://arxiv.org/abs/0901.0512).
- [4] F. Englert and R. Brout, *Broken symmetry and the mass of gauge vector mesons*, *Phys. Rev. Lett.* **13** (1964) 321.
- [5] P.W. Higgs, *Broken symmetries and the masses of gauge bosons*, *Phys. Rev. Lett.* **13** (1964) 508.

- [6] G. Guralnik, C. Hagen and T. Kibble, *Global conservation laws and massless particles*, *Phys. Rev. Lett.* **13** (1964) 585.
- [7] J. Adelman et al., *The silicon vertex trigger upgrade at CDF*, *Nucl. Instrum. Meth. A* **572** (2007) 361.
- [8] A. Annovi et al., *A VLSI processor for fast track finding based on content addressable memories*, *IEEE Trans. Nucl. Sci.* **53** (2006) 2428.
- [9] M. Dell’Orso and L. Ristori, *VLSI structures for track finding*, *Nucl. Instrum. Meth. A* **278** (1989) 436.
- [10] A. Annovi et al., *A new variable-resolution associative memory for high energy physics*, *Advancements in Nuclear Instrumentation Measurement Methods and their Applications (ANIMMA)*, 2011 2nd International Conference on Digital Object Identifier, *ANIMMA (2011)*.
- [11] A. Annovi et al., *The EDRO board connected to the associative memory “baby” fasttracker processor for the ATLAS experiment*, in 2nd International Conference on Technology and Instrumentation in Particle Physics, Chicago IL U.S.A. 9–14 June 2011.
- [12] A. Annovi and M. Beretta, *A fast general-purpose clustering algorithm based on FPGAs for high-throughput data processing*, *Nucl. Instrum. Meth. A* **617** (2010) 254 [[arXiv:0910.2572](#)].
- [13] A. Annovi et al., *Associative memory design for the Fast Tracker Processor (FTK) at ATLAS*, *IEEE Nucl. Sci. Symp. Med. Imag. Conf. (NSS/MIC)* (2011) 141.